Check for updates

Inhibition of glutaminase-1 in DLBCL potentiates venetoclax-induced antitumor activity by promoting oxidative stress

Beatriz Gomez Solsona,[1] Heike Horn,[2,3] Anja Schmitt,[4] Wendan Xu,[4] Philip Bucher,[1] Aylin Heinrich,[1] Sabrina Kalmbach,[2,3] Nina Kreienkamp,[4] Maik Franke,[4] Florian Wimmers,[1] Laurentz Schuhknecht,[5,6] Andreas Rosenwald,[7] Mattia Zampieri,[5,6] German Ott,[2] Georg Lenz,[4] Klaus Schulze-Osthoff,[1,8,9] and Stephan Hailfinger[4]

[1]Interfaculty Institute of Biochemistry, University of Tübingen, Tübingen, Germany; [2]Department of Clinical Pathology, Robert Bosch Hospital, Stuttgart, Germany; [3]Dr. Margarete Fischer Bosch Institute of Clinical Pharmacology, University of Tübingen, Stuttgart, Germany; [4]Department of Medicine A, Hematology, Oncology and Pneumology, University Hospital Münster, Münster, Germany; [5]Institute of Molecular Systems Biology, Department of Biology, ETH Zürich, Zürich, Switzerland; [6]Department of Biomedicine, University of Basel, Basel, Switzerland; [7]Institute of Pathology, University of Würzburg and Comprehensive Cancer Center Mainfranken, Würzburg, Germany; [8]German Cancer Consortium (DKTK) and German Cancer Research Center (DKFZ), Heidelberg, Germany; and [9]Cluster of Excellence iFIT (EXC 2180) "Image-Guided and Functionally Instructed Tumor Therapies," University of Tübingen, Tübingen, Germany

Key Points

- Genetic and pharmacological inhibition of GLS1 induces profound cytotoxicity in DLBCL cells independent of their subtype classification.

- Combination of ABT-199 with GLS1 inhibitors leads to synergistic killing by enhancing ROS accumulation.

Diffuse large B-cell lymphoma (DLBCL) is the most common lymphoma in adults, but first-line immunochemotherapy fails to produce a durable response in about one-third of the patients. Because tumor cells often reprogram their metabolism, we investigated the importance of glutaminolysis, a pathway converting glutamine to generate energy and various metabolites, for the growth of DLBCL cells. Glutaminase-1 (GLS1) expression was robustly detected in DLBCL biopsy samples and cell lines. Both pharmacological inhibition and genetic knockdown of GLS1 induced cell death in DLBCL cells regardless of their subtype classification, whereas primary B cells remained unaffected. Interestingly, GLS1 inhibition resulted not only in reduced levels of intermediates of the tricarboxylic acid cycle but also in a strong mitochondrial accumulation of reactive oxygen species. Supplementation of DLBCL cells with α-ketoglutarate or with the antioxidant α-tocopherol mitigated oxidative stress and abrogated cell death upon GLS1 inhibition, indicating an essential role of glutaminolysis in the protection from oxidative stress. Furthermore, the combination of the GLS1 inhibitor CB-839 with the therapeutic BCL2 inhibitor ABT-199 not only induced massive reactive oxygen species (ROS) production but also exhibited highly synergistic cytotoxicity, suggesting that simultaneous targeting of GLS1 and BCL2 could represent a novel therapeutic strategy for patients with DLBCL.

Introduction

Diffuse large B-cell lymphoma (DLBCL) constitutes the most prevalent lymphoma subtype in adults and is characterized by an aggressive clinical course.[1,2] Gene expression profiling and clustering of genetic aberrations revealed that DLBCL is a heterogeneous disease that can be classified into several molecular subtypes.[3-8] Gene expression profiling discriminates 2 major subtypes, the activated B

cell–like (ABC) and germinal center B cell–like (GCB) DLBCL. While GCB DLBCL frequently harbors mutations affecting *TP53*, *PTEN*, and *ING1*, ABC DLBCL is characterized by chronic B-cell receptor signaling owing to autoreactivity of the B-cell receptor or activating mutations, for example, of *CD79* or *CARD11*.[9] Although dual expression of c-Myc and BCL2 proteins is commonly observed in both DLBCL subtypes, it is associated with inferior clinical outcome only in GCB DLBCL.[10] First-line immunochemotherapy of DLCBL comprising the anti-CD20 antibody rituximab in combination with cyclophosphamide, hydroxydaunorubicin, vincristine (oncovin), and prednisolone (R-CHOP) achieves a durable response in around two-thirds of the patients with DLBCL.[1,2,9]

Tumor cells exhibit profound alterations in their metabolism. In addition to an abnormal glucose metabolism, many tumor cells have an increased glutamine metabolism to satisfy their increased demand of nucleotides, nonessential amino acids, and fatty acids. Glutamine is the most abundant amino acid in the blood and is taken up via various transporters, such as ASCT2 (SLC1A5) and members of the SLC38 family.[11] There are 2 major glutaminases (GLS), GLS1 and GLS2, which catalyze the conversion of glutamine to glutamate. GLS1 (also known as kidney-type GLS) is ubiquitously expressed and can be induced by oncogenes, such as c-Myc and c-Jun in cancer cells.[12,13] In contrast, the expression of GLS2 (also known as liver-type GLS) is restricted to the brain, liver, and pancreas and can be induced by the p53/p63/p73 family of transcription factors.[14-20] Although increased GLS1 expression often correlates with tumor growth and inferior patient survival, the role of GLS2 in cancer is less clear.[14] Several studies imply that GLS2 might act as a tumor suppressor, because it participates in the protection of cells from reactive oxygen species (ROS) and is able to induce a cell cycle arrest.[17,18,21]

Metabolic profiling revealed enhanced levels of glutaminolysis components in the plasma of patients suffering from aggressive lymphomas.[22] Moreover, several lymphoma cell lines are characterized by an increased glutaminolysis level associated with enhanced mitochondrial function and oxygen consumption rate.[23] Glutaminolysis can support the growth of tumor cells on several levels. On the one hand, deamination of glutamine to glutamate provides nitrogen required for the de novo synthesis of nucleotides and nonessential amino acids.[24] On the other hand, α-ketoglutarate, which is generated from glutamate by the activity of glutamate dehydrogenase or transaminases, serves as an anaplerotic substrate in the tricarboxylic acid cycle (TCA), thus helping the cancer cells meet their increased energy demand.[24,25] Moreover, α-ketoglutarate is a cosubstrate for dioxygenases, which mediate histone lysine and DNA cytosine demethylation, thereby connecting glutamine catabolism to the regulation of the epigenome.[26] Furthermore, under hypoxic conditions, glutamine-dependent reductive carboxylation fuels fatty acid synthesis, promotes lipid synthesis in fast-proliferating cells.[27-29] Glutamine plays an ambiguous role in maintaining the redox state of the cell. Due to its fueling of the TCA cycle and, thus, of the respiratory chain, not only oxygen consumption and adenosine triphosphate production are enhanced but also mitochondrial ROS production.[30] However, glutaminolysis also provides amino acids and reducing equivalents important for the biosynthesis and regeneration of antioxidative entities, such as glutathione.

Here, we investigated the role of GLS1, the key enzyme of glutamine catabolism, in DLBCL. We found that pharmacological inhibition or genetic depletion of GLS1 provoked the accumulation of ROS and induced cell death in preclinical DLBCL models. Both ROS formation and cell death were counteracted by the antioxidant α-tocopherol, suggesting that glutaminolysis is essential for the protection of DLBCL cells from oxidative cell death. Importantly, the combination of GLS1 inhibitors with the BCL2 inhibitor ABT-199 (venetoclax) further increased ROS generation and showed synergistic cytotoxicity, highlighting their potential for antilymphoma therapy.

Materials and methods

Cell culture, transfection, lentiviral, and retroviral transduction and survival assays

Protocols are provided in the supplemental Materials and Methods section.

Quantification of cellular glutathione levels

Levels of reduced glutathione (GSH) in cellular lysates were quantified using the GSH/GSSG-Glo Assay (Promega) according to the manufacturer's protocol.

Analysis of mitochondrial ROS

To monitor the accumulation of mitochondrial ROS, cells were stained with the mitochondria-specific superoxide sensor MitoSOX (Thermo Fisher Scientific). In brief, cells were washed once and then stained with 1 µM of MitoSOX in Hanks' balanced salt solution for 10 minutes at 37°C. After washing, dead cells were stained using SYTOX Blue dead cell stain (Thermo Fisher Scientific). The percentage of MitoSOX-positive cells and the mean fluorescence intensity of MitoSOX were quantified by flow cytometry (BD LSRII) and normalized to the mean fluorescence intensity of the solvent control probe.

Cell lysis and immunoblotting

Protocols are provided in the supplemental Materials and Methods section.

ELISA

Secreted interleukin-6 (IL-6) and IL-10 were quantified using human IL-6 and IL-10 enzyme-linked immunosorbent assay (ELISA) kits (Thermo Fisher Scientific), according to the manufacturer's protocol. To detect IL-6 in the U2932 cell line, the high-sensitivity IL-6 human ELISA kit was used (Thermo Fisher Scientific).

Immunohistochemistry, cell cycle analysis, apoptosis assay, and metabolomics

Protocols are provided in the supplemental Materials and Methods section.

## Results

GLS1 expression in DLBCL

To investigate whether GLS1 is essential for DLBCL survival, we analyzed its protein expression in a set of human DLBCL cell lines by immunoblotting and immunohistochemistry. All investigated DLBCL cell lines exhibited GLS1 expression, regardless of their classification as GCB or ABC DLBCL (Figure 1A-B). Compared

Figure 1. GLS1 expression in human DLBCL cell lines and biopsy samples. (A) GLS1, GLS2, and c-MYC protein expression in various ABC and GCB DLBCL cell lines was analyzed by immunoblotting. GAPDH served as loading control. Note that the protein doublet of the GLS1 blot might correspond to different GLS1 isoforms. (B) Immunohistochemical staining of GLS1 in human ABC and GCB DLBCL cell lines. Scale bars, 50 μm. (C) Immunohistochemical staining of GLS1 in human DLBCL biopsies (left pictures). The cytoplasmic GLS1 expression was quantified in DLBCL biopsy samples (n = 42, right panel).
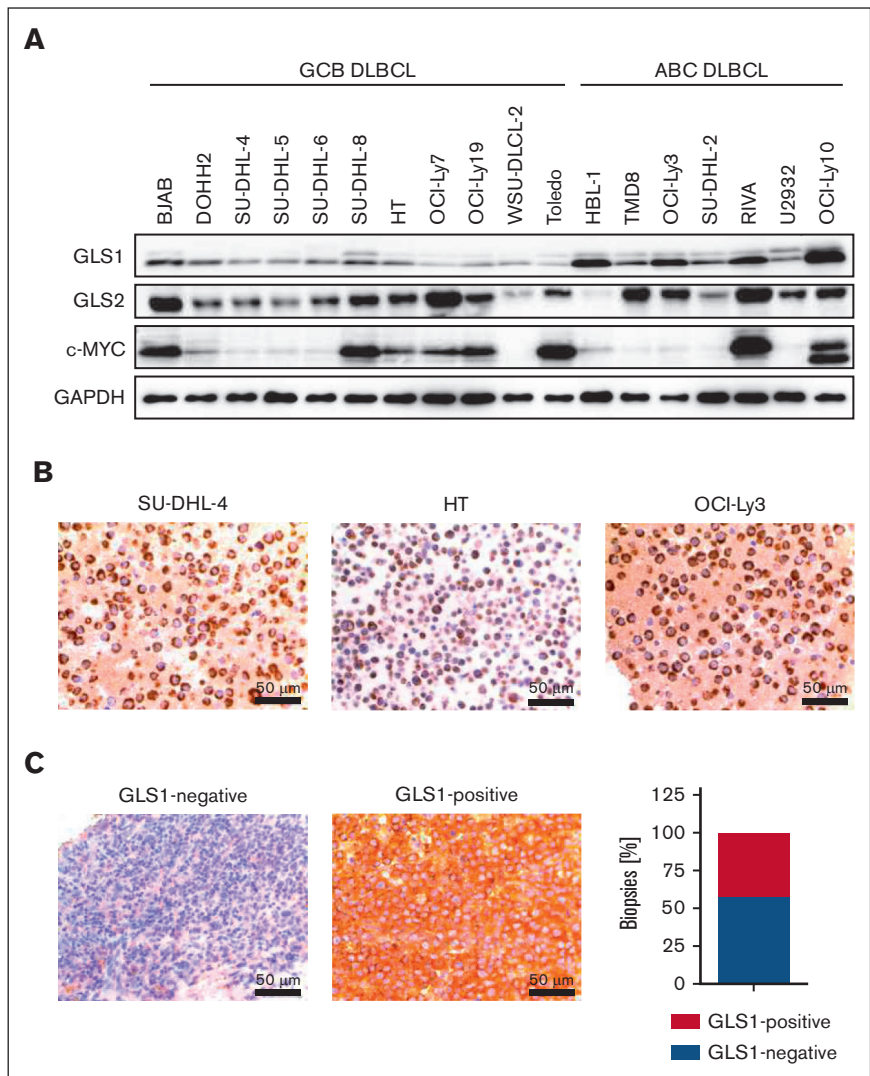
with DLBCL cell lines, human primary B cells only showed low GLS1 expression (supplemental Figure 1A). Because c-MYC is often deregulated in DLBCL and can drive GLS1 expression, we examined a potential correlation between c-MYC and GLS1 expression in DLBCL cell lines.[12,14] However, we were unable to detect a correlation between the c-MYC and GLS1 expression status in the DLBCL cell lines (Figure 1A). Accordingly, reduction of c-MYC expression using the BET inhibitor JQ1 did not alter GLS1 protein levels in various DLBCL cell lines (supplemental Figure 1B). To investigate GLS1 expression in primary DLBCL samples, we stained for GLS1 expression by immunohistochemistry in 42 human DLBCL biopsy samples. GLS1 expression was detected in 18 of 42 DLBCL biopsy samples (~43%) and was neither dependent on MYC status nor restricted to a certain DLBCL subtype (Figure 1C; supplemental Figure 1C).

Survival of DLBCL cells is dependent on GLS1 activity

To assess the importance of GLS1 activity for the survival of DLBCL cells, we treated the lymphoma cells for 6 days with CB-839 (telaglenastat), a specific GLS inhibitor that has shown promising efficacy in preclinical and clinical trials. At the nanomolar concentrations used, CB-839 has been reported to specifically target GLS1 but not GLS2.[31] Both ABC and GCB DLBCL cell lines were sensitive to the GLS1 inhibitor, whereas human primary B cells remained unaffected (Figure 2A-C; supplemental Figure 2A-C). Furthermore, IL-4/CD40L– or phytohemagglutinin– stimulated human primary B cells were largely resistant to CB-839 treatment, indicating that only transformed DLBCL cells depended on glutaminolysis (Figure 2C). CB-839 treatment only marginally affected the cell cycle of DLBCL cells; however, it rather potently induced cell death in the lymphoma cell lines (supplemental Figure 3A-B). To confirm that the observed cytotoxicity of CB-839 was indeed due to GLS1 inhibition, DLBCL cells were treated with BPTES, an allosteric GLS1 inhibitor, which also efficiently reduced the survival of all investigated DLBCL cell lines (Figure 3A-B). Moreover, short hairpin RNA–mediated knockdown of GLS, the gene encoding GLS1, in DOHH2 and HBL-1 cells resulted in an efficient reduction of GLS1 protein levels and impaired cell survival, an effect that was not observed in cells expressing a nontargeting vector control (Figure 3C-D).
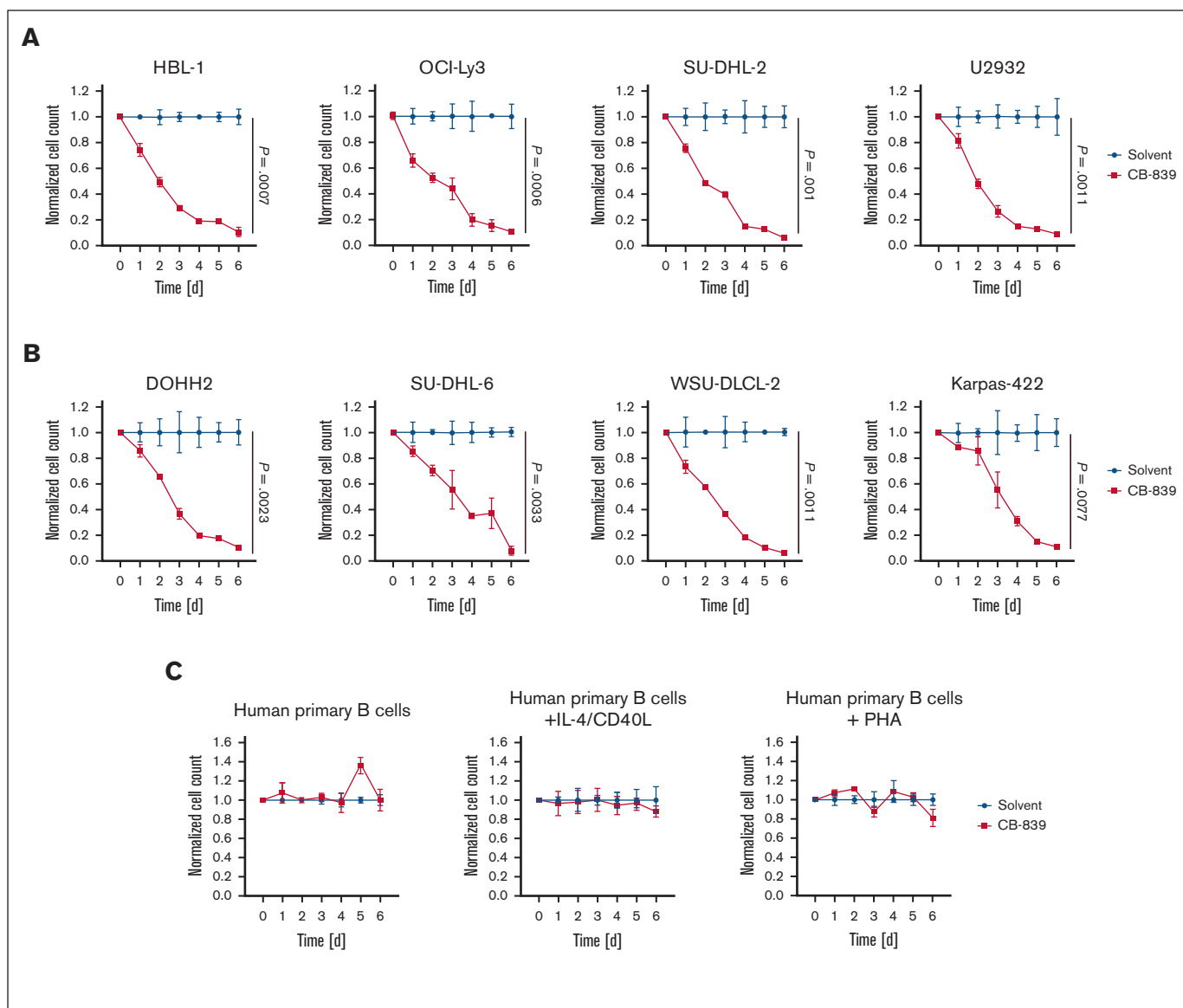
Figure 2. CB-839 induces cytotoxicity in DLBCL. Various ABC DLBCL cell lines (A), GCB DLBCL cell lines (B), or human primary B cells (C) were treated with solvent or 400 nM CB-839 and incubated for the indicated time. Cell numbers were determined daily and normalized to the solvent control. Error bars correspond to the mean ± standard deviation (SD). Data are representative of 3 for panels A-B or 2 for panel C independent experiments. (A-B) Statistical significance was calculated using the Student *t* test (unpaired, 2-tailed) to compare the solvent with the CB-839–treated samples at day 6.

Accordingly, the survival of the DLBCL cell lines was also impaired when the cells were cultivated in glutamine-free medium (Figure 3E). Collectively, we found that both ABC and GCB DLBCL cell lines are dependent on glutaminolysis and that targeting of GLS1 could provide a valid strategy for the treatment of patients with DLBCL.

CB-839 treatment reduces IL-6/IL-10 secretion

To investigate whether pharmacological inhibition of GLS1 affects signaling events crucial for DLBCL survival, the expression and phosphorylation of central regulators of the NF-κB, MAPK, AP-1, STAT3, and PI3K signaling pathways were analyzed by immunoblotting (Figure 4A; supplemental Figure 4). Although all signaling pathways investigated were largely unaffected, STAT3

phosphorylation was decreased upon CB-839 treatment.[32] Because ABC DLBCL cells are known to produce IL-6 and IL-10, which drive the auto/paracrine stimulation of the transformed B cells in a STAT-3-dependent manner, we quantified the secretion of these cytokines by ELISA. CB-839 treatment reduced IL-6 and IL-10 secretion, explaining the impaired STAT3 phosphorylation (Figure 4A-B). To investigate whether the reduced STAT3 activation determines the cytotoxicity of CB-839 in ABC DLBCL, we supplemented the medium with exogenous IL-6 and IL-10, which restored STAT3 phosphorylation, but was unable to alleviate the cytotoxicity of CB-839 (Figure 4A,C). Consistently, the inducible expression of a hyperactive STAT3 mutant (STAT3C) was not sufficient to protect the ABC DLBCL cell lines from CB-839-mediated toxicity, suggesting that the reduced activity of the
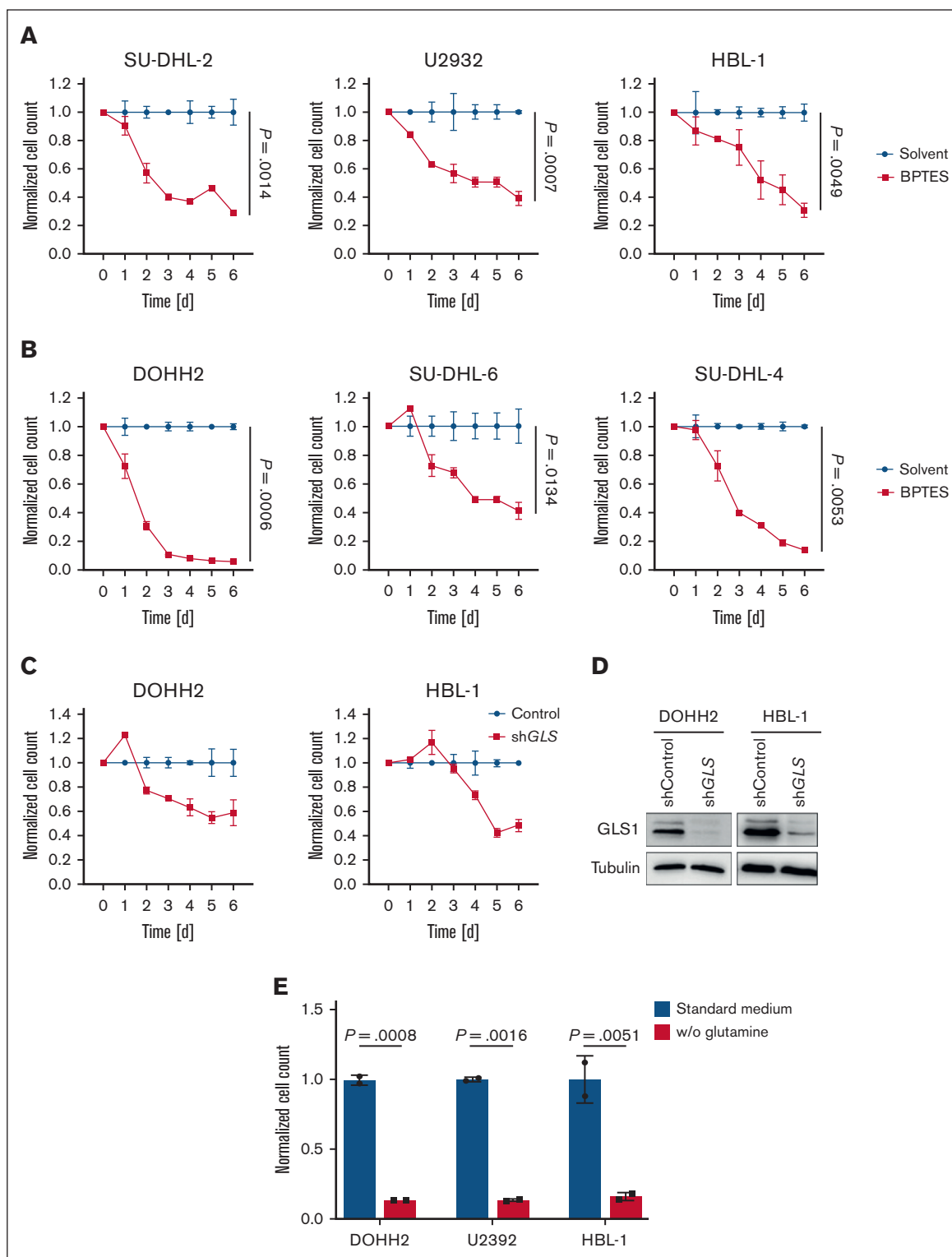
Figure 3. Glutaminolysis inhibition and glutamine deprivation impair DLBCL survival. Various ABC DLBCL cell lines (A) or GCB DLBCL cell lines (B) were treated with solvent or 1 μM BPTES. After the indicated time, cell numbers were determined and normalized to the solvent control. (C) DOHH2 and HBL-1 cells were transduced with either a nontargeting vector control or an short hairpin RNA (shRNA) targeting *GLS*. After transduction, cell numbers were determined daily as indicated and normalized to the nontargeting control. (D) The efficacy of the shRNA-mediated knockdown of GLS1 in DOHH2 and HBL-1 cells was controlled by immunoblotting. Tubulin served as a loading control. (E) ABC and GCB DLBCL cell lines were cultured in standard or glutamine-deprived medium for 5 days. Cell numbers were determined and normalized to the standard medium control. Error bars correspond to the mean ± SD. Data are representative of 3 for panels A-B or 2 for panels C-E independent experiments. (A-B) Statistical significance was calculated using the Student *t* test (unpaired, 2-tailed) to compare the solvent with the BPTES-treated samples at day 6.
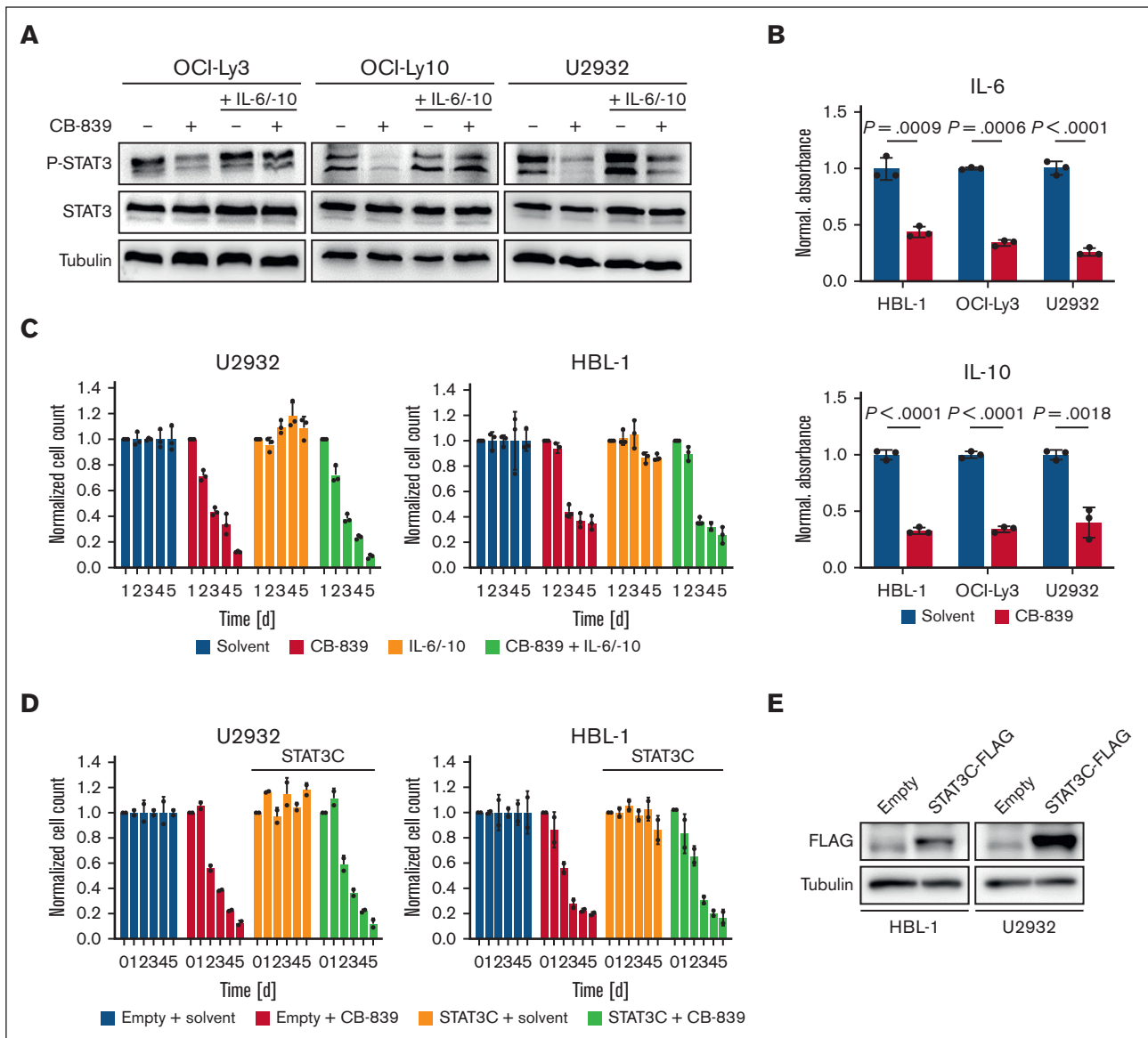
Figure 4. CB-839 reduces IL-6/IL-10 secretion and impairs STAT3 activation. (A) ABC DLBCL cell lines were treated with solvent, 500 nM CB-839 and/or 5 ng/mL recombinant human IL-6 and IL-10, as indicated, and the phosphorylation of STAT3 was assessed by immunoblot analysis. Tubulin served as loading control. (B) ABC DLBCL cell lines were treated with solvent or 500 nM CB-839 for 48 hours. Secreted IL-6 and IL-10 were quantified by ELISA and normalized to the solvent control. (C) The ABC DLBCL cell lines HBL-1 and U2932 were treated with solvent, 500 nM CB-839 and/or 5 ng/mL recombinant human IL-6 and IL-10, as indicated. Cell numbers were determined daily and normalized to the solvent control. (D-E) HBL-1 and U2932 cells expressing an inducible control vector or the hyperactive mutant STAT3C-FLAG were treated with 1 μg/mL doxycycline to induce cDNA expression for 24 hours. Cells were then treated with solvent or 500 nM CB-839. Cell numbers were quantified at the indicated times and normalized to the respective solvent controls. Error bars correspond to the mean ± SD. Data are representative of 3 for panels B-C or 2 for panels A,D-E independent experiments. Statistical significance was calculated using the Student *t* test (unpaired, 2-tailed) to compare the solvent with the CB-839–treated samples. cDNA, complementary DNA.

STAT3 pathway is not the major driver for the antilymphoma effect of the glutaminolysis inhibitor (Figure 4D-E).

GLS1 inhibition provokes oxidative stress in DLBCL

To gain a deeper mechanistic insight into the metabolic pathways affected by GLS1 inhibition in DLBCL, we analyzed the metabolome of CB-839–treated and control cells by mass spectrometry. As expected, an accumulation of glutamine and a concomitant reduction of glutamate and α-ketoglutarate could be observed upon CB-839 treatment (Figure 5A). We noticed that several

intermediates of the TCA cycle were among the metabolites most strongly reduced upon GLS1 inhibition, whereas other metabolic pathways seemed unaffected (Figure 5A; supplemental Figure 5A). To investigate whether the importance of glutaminolysis for the growth of DLBCL is based on its role to fuel the TCA cycle or rather to provide nitrogen for the synthesis of purines/pyrimidines and nonessential amino acids, we supplemented CB-839–treated cells with a dimethylated and hence membrane-permeable form of α-ketoglutarate. Supplementation with α-ketoglutarate indeed mitigated the cytotoxic effect of CB-839 in various DLBCL cell
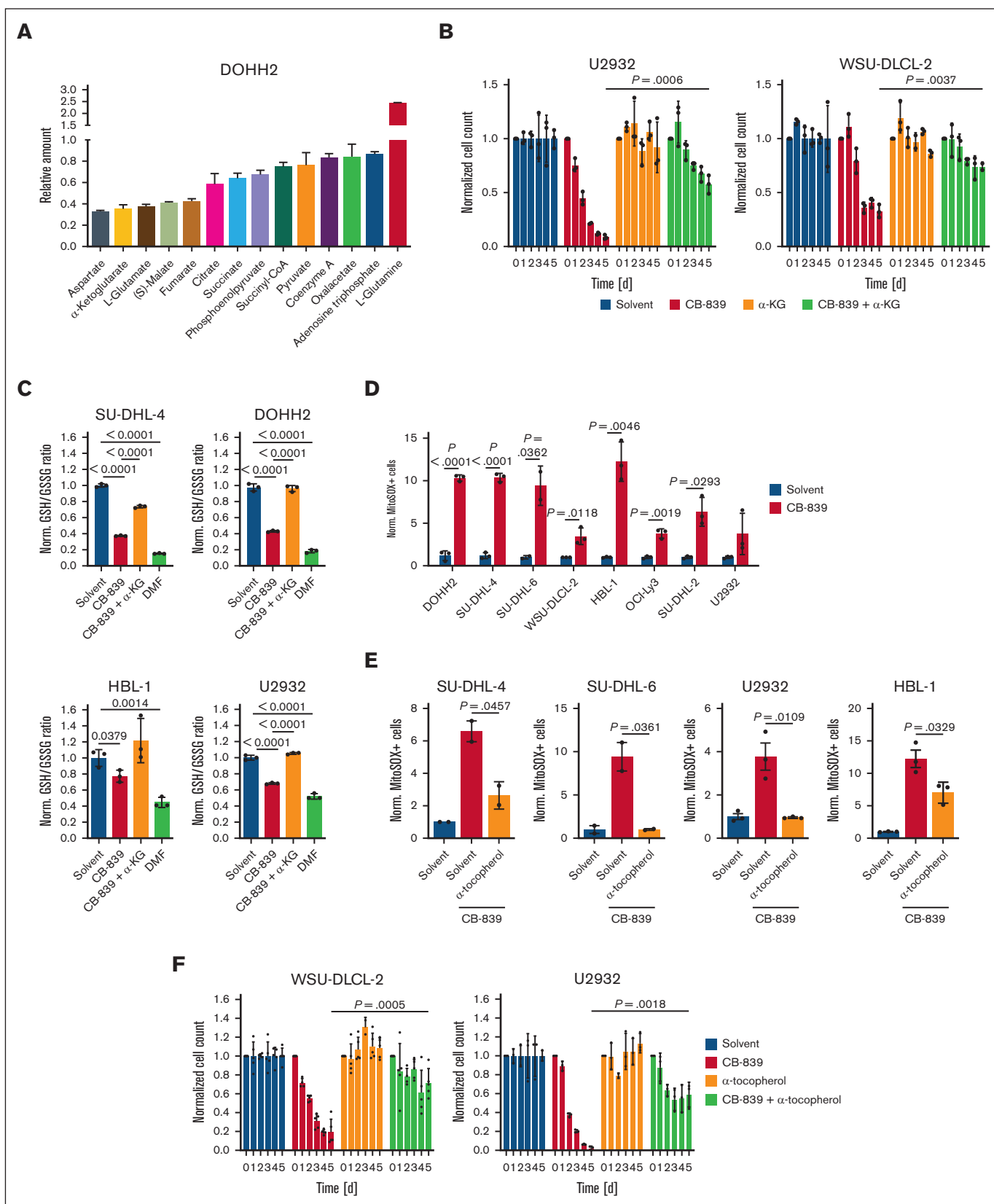
Figure 5. GLS1 inhibition induces mitochondrial ROS formation and reduces GSH levels in DLBCL cells. (A) DOHH2 cells were treated with solvent or 500 nM CB-839 for 48 hours. Metabolites were analyzed and quantified by mass spectrometry and normalized to the solvent control. (B) DLBCL cells were treated with solvent or 500 nM

lines, indicating that glutamine is not primarily crucial as a nitrogen donor in DLBCL (Figure 5B; supplemental Figure 5B).

Although the moderate reduction of adenosine triphosphate levels indicated that the GLS1 blockade does not primarily impair the cellular energy supply, we noticed that several antioxidative entities, such as GSH, α-tocopherol, and reduced nicotinamide adenine dinucleotide phosphate were impaired upon CB-839 treatment (Figure 5A,C; supplemental Figure 5C). Interestingly, supplementation of α-ketoglutarate was sufficient to restore the ratio of reduced/oxidized glutathione after CB-839 treatment to the levels of solvent-treated cells, indicating that glutaminolysis plays an important role in the control of the cellular redox state (Figure 5C; supplemental Figure 5D). To assess whether the inhibition of glutaminolysis is sufficient to induce the accumulation of ROS in DLBCL, we quantified mitochondrial ROS by flow cytometry using the fluorescent probe MitoSOX. In all investigated DLBCL cell lines, CB-839 treatment resulted in increased ROS levels after 48 hours (Figure 5D). We screened several antioxidants for their ability to prevent mitochondrial ROS accumulation and observed that α-tocopherol was capable of significantly reducing ROS levels induced by CB-839 treatment (Figure 5E; supplemental Figure 6A). To investigate whether CB-839-dependent ROS production contributes to its cytotoxic function, we supplemented GLS1-inhibited DLBCL cell lines with α-tocopherol. Strikingly, α-tocopherol significantly alleviated the cytotoxicity of CB-839, indicating that ROS accumulation induced by GLS1 inhibition contributes substantially to its antilymphoma effect (Figure 5F; supplemental Figure 6B-C). Because α-tocopherol has been described as a potent ferroptosis inhibitor, we analyzed whether lipid peroxidation, a hallmark of ferroptosis, was detectable upon CB-839 treatment. Although the ferroptosis inducer dimethyl fumarate induced robust lipid peroxidation in the lymphoma cell lines, GLS1 inhibition did not provoke the peroxidation of lipids (supplemental Figure 6D).

GLS1 inhibition acts synergistically with the BCL2 inhibitor ABT-199 in ROS generation and killing of DLBCL

We hypothesized that combinatorial treatment with the GLS1 inhibitor CB-839 and another compound that promotes ROS accumulation would result in the synergistic killing of DLBCL cells. The BCL2 inhibitor ABT-199 (venetoclax) has previously been demonstrated to disrupt respiratory chain supercomplex formation, thereby inducing ROS production in T cells.[33,34] Indeed, the single treatment of DLBCL cells with ABT-199 increased ROS levels in a dose-dependent manner (supplemental Figure 7A). Although single treatment with CB-839 or ABT-199 resulted in a robust but moderate ROS induction, the combination of both drugs caused

an excessive ROS accumulation in various DLBCL cell lines (Figure 6A). Accordingly, simultaneous treatment of DLBCL with CB-839 and ABT-199 resulted in an enhanced cytotoxicity compared with the respective single treatments (Figure 6B; supplemental Figure 7B). Using the Loewe additivity model, we were able to demonstrate that the combination of CB-839 and ABT-199 resulted in synergistic cytotoxicity over various concentrations, indicating that this combinatorial treatment might represent a promising strategy for treating DLBCL (Figure 6C; supplemental Figure 7C).

Discussion

Because various cancer cells use glutaminolysis to satisfy their increased demand for energy, nonessential amino acids, nucleotides, and fatty acids, pharmacological targeting of GLS1 has been proposed as a promising strategy for anticancer treatment and is currently tested in clinical trials.[14,24] The blockade of GLS activity results in variable outcomes in different cancer types, most likely dependent on the expression status of different GLS isoforms and the metabolic addiction or specific resistance mechanisms.[14] Here, to the best of our knowledge, we describe for the first time that all DLBCL cell lines investigated express GLS1 regardless of their subtype classification.

So far, it remains unclear how GLS1 expression is driven in DLBCL. c-MYC has previously been identified to be the main regulator of GLS1 transcription because it suppresses the expression of miR-23a/b that targets the GLS 3'-untranslated region.[12] Because c-MYC activation is, due to MYC amplifications and translocations, a common event in DLBCL, we speculated that c-MYC signaling regulates GLS1 expression. However, because we could not detect any correlation between the expression of c-MYC and GLS1 and because JQ1-mediated reduction of c-MYC expression did not lower GLS1 protein levels, other transcription factors are likely to be responsible for the GLS1 expression observed in DLBCL.[35] Xia et al reported that the protease activity of the NF-κB activator MALT1 promotes the expression of GLS1.[32] Because MALT1 is only active in the ABC DLBCL subtype but GLS1 expression could be detected in all DLBCL subtypes, it is unlikely that MALT1 serves as a general GLS1-inducer in DLBCL.[36,37] Although all investigated DLBCL cell lines expressed GLS1, we detected GLS1 expression in only 43% of the DLBCL biopsy samples. This suggests that either GLS1+ DLBCL cells are more suitable for in vitro cultivation or tumor cells adapt to the glutamine supply in culture. Furthermore, we were unable to detect GLS2 expression in DLBCL biopsy samples, suggesting that GLS1 is the main driver of glutaminolysis in DLBCL. Thus, in future clinical trials, GLS1 expression in DLBCL biopsy samples should be monitored before GLS1 inhibitor treatment.

Figure 5 (continued) CB-839 alone or in combination with 0.5 mM of membrane-permeable α-ketoglutarate (α-KG) for 5 days. Cell numbers were determined as indicated and normalized to the solvent control. (C) The indicated DLBCL cell lines were treated with the GSH-depleting agent DMF (20 μM) or 500 nM CB-839 for 24 hours alone or in combination with 0.5 mM membrane-permeable α-KG. The ratio of reduced to oxidized glutathione was determined and normalized to the respective solvent-treated controls. (D-E) DLBCL cells were treated for 48 hours with solvent or 500 nM CB-839 alone (D) or in combination with 100 μM α-tocopherol (E) before analysis of superoxide formation by flow cytometry using MitoSOX. The percentage of MitoSOX-positive cells in CB-839-treated samples was normalized to the solvent control. (F) WSU-DLCL-2 and U2932 cells were treated with solvent or 500 nM CB-839, alone or in combination with 100 μM α-tocopherol for 5 days. Cell numbers were determined as indicated and normalized to the solvent control. Error bars correspond to the mean ± SD. Data are representative of 3 independent experiments for panels A-F. (B-F) Statistical significance was calculated using the Student t test (unpaired, 2-tailed) to compare the indicated samples. DMF, dimethyl fumarate.
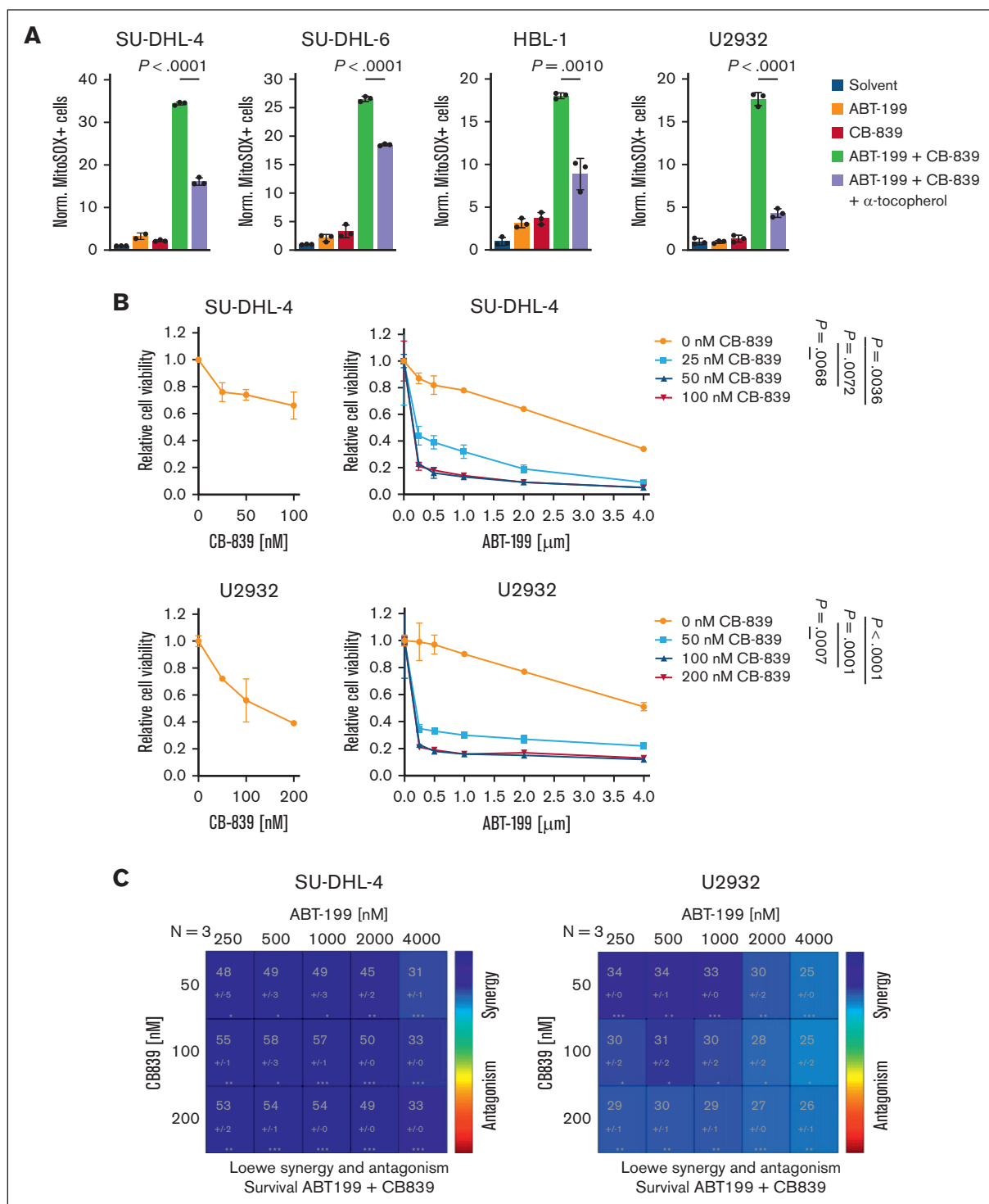
Figure 6. Synergistic killing of DLBCL cells by the combined inhibition of GLS1 and BCL2. (A) DLBCL cells were treated for 48 hours with solvent, 0.5 µM ABT-199, or 250 nM CB-839 alone or in combination, with or without 100 µM α-tocopherol. Mitochondrial ROS were then quantified by flow cytometry. The percentage of MitoSOX-positive cells of CB-839–treated samples was normalized to the solvent control. (B) SU-DHL-4 and U2932 cells were treated with CB-839 alone (left panels) or in combination with ABT-199 (right panels). Cell survival was quantified by MTS assay after 48 hours, and combination treatments were normalized to the respective CB-839 single treatment. Statistical significance was calculated by comparing the data points of the solvent control with the CB839-treated samples in presence of 4 µM ABT-199. (C) The Loewe additivity model was used to identify synergism between the CB-839 and ABT-199 doses assayed. Error bars correspond to the mean ± SD. Data are representative of 3 for panels A-B independent experiments. Statistical significance was calculated using the Student t test (unpaired, 2-tailed) to compare the indicated samples. MTS, 3-(4,5-dimethylthiazol-2-yl)-5-(3-carboxymethoxyphenyl)-2-(4-sulfophenyl)-2H-tetrazolium.

Surprisingly, we found that the cytotoxicity of the GLS1 inhibitor CB-839 was largely mediated by ROS induction rather than by a decreased energy metabolism or restricted supply of amino acids and nucleotides. Upon GLS1 inhibition, impaired levels of the antioxidant glutathione were detected, which could be explained on at least 2 levels. First, glutamate is not only a direct precursor of glutathione, but also serves as a cofactor in the import of cystine, another essential glutathione precursor, via the system x_c^- glutamate/cystine antiporter.[38] Second, glutamine-derived α-ketoglutarate replenishes the TCA cycle and contributes to the generation of reducing equivalents serving as cofactors for glutathione reductase.[39,40] Because we detected a decreased ratio of reduced to oxidized glutathione as well as lower levels of the reduced forms of other antioxidants, such as α-tocopherol, in the GLS1 inhibitor–treated cells, we propose that the reductive capacity to regenerate these antioxidants is impaired upon GLS1 inhibition in DLBCL. Accordingly, replenishing the TCA cycle upon CB-839 treatment by α-ketoglutarate supplementation did not only alleviate the cytotoxic effect of CB-839 but also restored the cellular pool of GSH.

The increased ROS levels observed upon inhibition of glutaminolysis can not only be detected in DLBCL but have been described in various cancers, such as acute myeloid leukemia or head and neck squamous cell carcinoma.[14,41,42] Because the lipophilic antioxidant α-tocopherol alleviated CB-839–mediated ROS accumulation and represents a potent inhibitor of ferroptosis, an oxidative form of cell death, we investigated whether GLS1 inhibition triggers ferroptosis in DLBCL cell lines. A hallmark of ferroptosis is excessive lipid peroxidation, which we detected after treatment with the ferroptosis inducer dimethyl fumarate but not upon CB-839 exposure, suggesting that the CB-839–mediated cell death cannot be characterized as classical ferroptosis.[43] Interestingly, oxidative stressors such as arsenic trioxide have been described to enhance the efficacy of GLS1 inhibition in acute myeloid leukemia, suggesting that boosting ROS generation in tumor cells by combinatorial treatments might represent an interesting therapeutic strategy.[41]

Indeed, we found that combination of CB-839 with ABT-199, a BCL2 inhibitor currently approved and used for the treatment of different hematological malignancies, strongly enhanced the induction of cell death in DLBCL. We propose to combine GLS1 inhibitors with ABT-199 because of 2 reasons. First, because overexpression of BCL2 is a common event in DLBCL, ABT-199 can directly target this major antiapoptotic mechanism in DLBCL cells.[44-46] Second, ABT-199 has been shown to provoke ROS formation in T cells by preventing the assembly of respiratory chain supercomplexes[33,34] and hence can be assumed to cooperate with CB-839 in ROS generation.[33,34] Indeed, combinatorial treatment of DLBCL cells with ABT-199 and CB-839 resulted in synergistic ROS formation and cytotoxicity. Interestingly, it has been recently reported that ABT-199 promoted the efficacy of CB-839 also in mantle cell lymphoma.[47] Collectively, to the best of our knowledge, we describe here for the first time that DLBCL cells are dependent on glutaminolysis and that the combination of CB-839 with ABT-199 might represent an interesting strategy to therapeutically target DLBCL.

Acknowledgments

Authorship

Contribution: B.G.S., H.H., A.S., W.X., P.B., A.H., S.K., N.K., M.F., and L.S. performed experiments; B.G.S., A.R., F.W., M.Z., G.O., G.L., K.S.-O., and S.H. analyzed data; B.G.S. and S.H. wrote the manuscript, which all other authors commented on; and G.L., K.S.-O., and S.H. conceived and coordinated the study.

Conflict-of-interest disclosure: G.L. has participated in a consulting or advisory role not related to the results of this study for AbbVie, ADC Therapeutics, Amgen, AstraZeneca, Bayer, Bristol Myers Squibb, Constellation, Gilead, Genase, Genmab, Hexal/Sandoz, Immagene, Incyte, Janssen, Karyopharm, Lilly, Miltenyi, MorphoSys, NanoString, Novartis, PentixaPharm, Roche, Sobi, and Takeda; has been on a speaker's bureau for Bayer, Celgene, Gilead, Janssen and Roche; and has received research funding not related to this study from Aquinox, AstraZeneca, Bayer, Celgene, Gilead, Janssen, and Roche. The remaining authors declare no competing financial interests.

Correspondence: Stephan Hailfinger, Translational Oncology, Department of Medicine A, University Hospital Münster, Domagkstr. 3, 48149 Münster, Germany; email: stephan.hailfinger@ukmuenster.de.

References

1. Swerdlow SH, Campo E, Pileri SA, et al. The 2016 revision of the World Health Organization classification of lymphoid neoplasms. *Blood*. 2016; 127(20):2375-2390.

2. Nogai H, Dörken B, Lenz G. Pathogenesis of non-Hodgkin's lymphoma. *J Clin Oncol*. 2011;29(14):1803-1811.

3. Alizadeh AA, Eisen MB, Davis RE, et al. Distinct types of diffuse large B-cell lymphoma identified by gene expression profiling. *Nature*. 2000;403(6769):503-511.

4. Rosenwald A, Wright G, Chan WC, et al. The use of molecular profiling to predict survival after chemotherapy for diffuse large-B-cell lymphoma. *N Engl J Med*. 2002;346(25):1937-1947.

5. Wright GW, Huang DW, Phelan JD, et al. A probabilistic classification tool for genetic subtypes of diffuse large B cell lymphoma with therapeutic implications. *Cancer Cell*. 2020;37(4):551-568.e14.

6. Wright G, Tan B, Rosenwald A, Hurt EH, Wiestner A, Staudt LM. A gene expression-based method to diagnose clinically distinct subgroups of diffuse large B cell lymphoma. *Proc Natl Acad Sci U S A*. 2003;100(17):9991-9996.

7. Chapuy B, Stewart C, Dunford AJ, et al. Molecular subtypes of diffuse large B cell lymphoma are associated with distinct pathogenic mechanisms and outcomes. *Nat Med*. 2018;24(5):679-690.

8. Schmitz R, Wright GW, Huang DW, et al. Genetics and pathogenesis of diffuse large B-cell lymphoma. *N Engl J Med*. 2018;378(15):1396-1407.

9. Pasqualucci L, Dalla-Favera R. Genetics of diffuse large B-cell lymphoma. *Blood*. 2018;131(21):2307-2319.

10. Staiger AM, Ziepert M, Horn H, et al. Clinical impact of the cell-of-origin classification and the MYC/ BCL2 dual expresser status in diffuse large B-cell lymphoma treated within prospective clinical trials of the German High-Grade Non-Hodgkin's Lymphoma Study Group. *J Clin Oncol*. 2017;35(22): 2515-2526.

11. Bhutia YD, Ganapathy V. Glutamine transporters in mammalian cells and their functions in physiology and cancer. *Biochim Biophys Acta*. 2016; 1863(10):2531-2539.

12. Gao P, Tchernyshyov I, Chang TC, et al. c-Myc suppression of miR-23a/b enhances mitochondrial glutaminase expression and glutamine metabolism. *Nature*. 2009;458(7239):762-765.

13. Momcilovic M, Bailey ST, Lee JT, et al. The GSK3 signaling axis regulates adaptive glutamine metabolism in lung squamous cell carcinoma. *Cancer Cell*. 2018;33(5):905-921.e5.

14. Wang Z, Liu F, Fan N, et al. Targeting glutaminolysis: new perspectives to understand cancer development and novel strategies for potential target therapies. *Front Oncol*. 2020;10:589508.

15. Saha SK, Islam SMR, Abdullah-Al-Wadud M, Islam S, Ali F, Park KS. Multiomics analysis reveals that GLS and GLS2 differentially modulate the clinical outcomes of cancer. *J Clin Med*. 2019;8(3):355.

16. GTEx Consortium. Human genomics. The Genotype-Tissue Expression (GTEx) pilot analysis: multitissue gene regulation in humans. *Science*. 2015; 348(6235):648-660.

17. Suzuki S, Tanaka T, Poyurovsky MV, et al. Phosphate-activated glutaminase (GLS2), a p53-inducible regulator of glutamine metabolism and reactive oxygen species. *Proc Natl Acad Sci U S A*. 2010;107(16):7461-7466.

18. Hu W, Zhang C, Wu R, Sun Y, Levine A, Feng Z. Glutaminase 2, a novel p53 target gene regulating energy metabolism and antioxidant function. *Proc Natl Acad Sci U S A*. 2010;107(16):7455-7460.

19. Giacobbe A, Bongiorno-Borbone L, Bernassola F, et al. p63 regulates glutaminase 2 expression. *Cell Cycle*. 2013;12(9):1395-1405.

20. Velletri T, Romeo F, Tucci P, et al. GLS2 is transcriptionally regulated by p73 and contributes to neuronal differentiation. *Cell Cycle*. 2013;12(22): 3564-3573.

21. Matés JM, Segura JA, Martín-Rufián M, Campos-Sandoval JA, Alonso FJ, Márquez J. Glutaminase isoenzymes as key regulators in metabolic and oxidative stress against cancer. *Curr Mol Med*. 2013;13(4):514-534.

22. Barberini L, Noto A, Fattuoni C, et al. The metabolomic profile of lymphoma subtypes: a pilot study. *Molecules*. 2019;24(13):2367.

23. Liu X, Wang L, Jiang W, Lu W, Yang J, Yang W. B cell lymphoma with different metabolic characteristics show distinct sensitivities to metabolic inhibitors. *J Cancer*. 2018;9(9):1582-1591.

24. Yang L, Venneti S, Nagrath D. Glutaminolysis: a hallmark of cancer metabolism. *Annu Rev Biomed Eng*. 2017;19:163-194.

25. DeBerardinis RJ, Mancuso A, Daikhin E, et al. Beyond aerobic glycolysis: transformed cells can engage in glutamine metabolism that exceeds the requirement for protein and nucleotide synthesis. *Proc Natl Acad Sci U S A*. 2007;104(49):19345-19350.

26. Islam MS, Leissing TM, Chowdhury R, Hopkinson RJ, Schofield CJ. 2-oxoglutarate-dependent oxygenases. *Annu Rev Biochem*. 2018;87:585-620.

27. Dang L, White DW, Gross S, et al. Cancer-associated IDH1 mutations produce 2-hydroxyglutarate. *Nature*. 2009;462(7274):739-744.

28. Jiang L, Shestov AA, Swain P, et al. Reductive carboxylation supports redox homeostasis during anchorage-independent growth. *Nature*. 2016; 532(7598):255-258.

29. Metallo CM, Gameiro PA, Bell EL, et al. Reductive glutamine metabolism by IDH1 mediates lipogenesis under hypoxia. *Nature*. 2011;481(7381): 380-384.

30. Weinberg F, Hamanaka R, Wheaton WW, et al. Mitochondrial metabolism and ROS generation are essential for Kras-mediated tumorigenicity. *Proc Natl Acad Sci U S A*. 2010;107(19):8788-8793.

31. Gross MI, Demo SD, Dennison JB, et al. Antitumor activity of the glutaminase inhibitor CB-839 in triple-negative breast cancer. *Mol Cancer Ther*. 2014; 13(4):890-901.

32. Xia X, Zhou W, Guo C, et al. Glutaminolysis mediated by MALT1 protease activity facilitates PD-L1 expression on ABC-DLBCL cells and contributes to their immune evasion. *Front Oncol*. 2018;8:632.

33. Nguyen LXT, Troadec E, Kalvala A, et al. The Bcl-2 inhibitor venetoclax inhibits Nrf2 antioxidant pathway activation induced by hypomethylating agents in AML. *J Cell Physiol*. 2019;234(8):14040-14049.

34. Lee JB, Khan DH, Hurren R, et al. Venetoclax enhances T cell-mediated antileukemic activity by increasing ROS production. *Blood*. 2021;138(3): 234-245.

35. Xia Y, Zhang X. The spectrum of MYC alterations in diffuse large B-cell lymphoma. *Acta Haematol*. 2020;143(6):520-528.

36. Hailfinger S, Lenz G, Ngo V, et al. Essential role of MALT1 protease activity in activated B cell-like diffuse large B-cell lymphoma. *Proc Natl Acad Sci U S A*. 2009;106(47):19946-19951.

37. Ferch U, Kloo B, Gewies A, et al. Inhibition of MALT1 protease activity is selectively toxic for activated B cell-like diffuse large B cell lymphoma cells. *J Exp Med*. 2009;206(11):2313-2320.

38. Lewerenz J, Hewett SJ, Huang Y, et al. The cystine/glutamate antiporter system x(c)(-) in health and disease: from molecular mechanisms to novel therapeutic opportunities. *Antioxid Redox Signal*. 2013;18(5):522-555.

39. Son J, Lyssiotis CA, Ying H, et al. Glutamine supports pancreatic cancer growth through a KRAS-regulated metabolic pathway. *Nature*. 2013; 496(7443):101-105.

40. Gansemer ER, McCommis KS, Martino M, et al. NADPH and glutathione redox link TCA cycle activity to endoplasmic reticulum homeostasis. *iScience*. 2020;23(5):101116.

41. Gregory MA, Nemkov T, Park HJ, et al. Targeting glutamine metabolism and redox state for leukemia therapy. *Clin Cancer Res*. 2019;25(13): 4079-4090.

42. Wicker CA, Hunt BG, Krishnan S, et al. Glutaminase inhibition with telaglenastat (CB-839) improves treatment response in combination with ionizing radiation in head and neck squamous cell carcinoma models. *Cancer Lett*. 2021;502:180-188.

43. Schmitt A, Xu W, Bucher P, et al. Dimethyl fumarate induces ferroptosis and impairs NF-κB/STAT3 signaling in DLBCL. *Blood*. 2021;138(10):871-884.

44. Tsuyama N, Sakata S, Baba S, et al. BCL2 expression in DLBCL: reappraisal of immunohistochemistry with new criteria for therapeutic biomarker evaluation. *Blood*. 2017;130(4):489-500.

45. Li L, Pongtornpipat P, Tiutan T, et al. Synergistic induction of apoptosis in high-risk DLBCL by BCL2 inhibition with ABT-199 combined with pharmacologic loss of MCL1. *Leukemia*. 2015;29(8):1702-1712.

46. Li Q, Cheng L, Shen K, et al. Efficacy and safety of Bcl-2 inhibitor venetoclax in hematological malignancy: a systematic review and meta-analysis of clinical trials. *Front Pharmacol*. 2019;10:697.

47. Li L, Nie L, Jordan A, et al. Targeting glutaminase is therapeutically effective in ibrutinib-resistant mantle cell lymphoma. *Haematologica*. 2023;108(6): 1616-1627.